International Symposium
On Turbulence and Shear Flow
Phenomena (TSFP-9)
June 30 - July 3, 2015 *Melbourne, Australia*

COHERENT VORTICITY IN TURBULENT CHANNEL FLOW: A WAVELET VIEWPOINT

K. Yoshimatsu
EcoTopia Science Institute
Nagoya University
Nagoya, 464-8603, Japan
yoshimatsu.katsunori@g.mbox.nagoya-u.ac.jp

T. Sakurai
Department of Computational Science and Engineering
Nagoya University
Nagoya, 464-8603, Japan
sakurai@fluid.cse.nagoya-u.ac.jp

K. Schneider
M2P2-CNRS and CMI
Aix-Marseille Université
38 rue F. Joliot-Curie, 13451 Marseille Cedex 20, France
kschneid@cmi.univ-mrs.fr

M. Farge
LMD-IPSL-CNRS
Ecole Normale Supérieure
24 rue Lhomond, 75231 Paris Cedex 05, France
farge@lmd.ens.fr

K. Morishita
Education Center on Computational Science and Engineering
Kobe University
Kobe, 650-0047, Japan
morishita@port.kobe-u.ac.jp

T. Ishihara
Center for Computational Science
Nagoya University
Nagoya, 464-8603, Japan
ishihara@cse.nagoya-u.ac.jp

INTRODUCTION

Turbulent flows exhibit an intrinsic multiscale behavior and are characterized by a large number of degrees of freedom interacting nonlinearly. Observations, even at large Reynolds number, show self-organization of the flow into coherent vortices (Brown and Roshko, 1974), which are superimposed to a random background flow (She et al., 1991). This motivates to split turbulent flows into these two contributions, which are both multiscale and exhibit no scale separation. Multiscale decompositions, such as wavelet bases, are suitable tools for extracting coherent vortices. The simultaneous scale and space localization of wavelets allows an efficient representation of such intermittent data. In particular, orthogonal wavelets allow fast wavelet transformation. Using orthogonal wavelets, a coherent vorticity extraction method was proposed for isotropic turbulence by Farge et al. (2001). It has been applied to different types of hydrodynamic turbulent flows, e.g., mixing layers (Schneider et al., 2005) and boundary layers (Khujadze et al., 2011), which present turbulent and non-turbulent regions.

The extraction is performed in wavelet space. The flow vorticity is decomposed into an orthogonal wavelet series and we apply a thresholding to split the coefficients into two sets. The coherent vorticity, reconstructed from the few strongest wavelet coefficients, well preserves the total turbulent statistics, while the incoherent vorticity, reconstructed from the remaining large majority of the coefficients that are very weak, corresponds to a noise-like background flow. The coherent and incoherent velocity fields are reconstructed from the coherent and incoherent vorticity fields, respectively, using the Biot-Savart relation. Thus, we can efficiently examine the role of coherent vorticity in

turbulence. Other conventional methods to identify organized vortices in turbulence, such as the Q-criterion and λ_2 method (Jeong et al., 1997), have difficulties to get scale information of the vortices and analyze precisely the contribution of the coherent vorticity. Since those methods work in physical space, they do not preserve the smoothness of the vorticity they extract due to edge effects.

In the present work, we consider a turbulent channel flow bounded by two parallel walls. For coherent vorticity extraction, we propose an anisotropic wavelet decomposition which allows us to take into account the no-slip boundary condition at the walls. Statistical analyses of the coherent and incoherent flow contributions are performed and compared with those of the total flow. In particular the contribution of the coherent flow onto the nonlinear dynamics is assessed. This is the first case for the extraction method using orthogonal wavelets to take the solid boundary into account, and to obtain these contributions.

METHODOLOGY

We analyze direct numerical simulation (DNS) data of a fully developed turbulent channel flow at friction-velocity based Reynolds number $Re_\tau = 320$ (Morishita et al., 2011). Here, $Re_\tau = u_\tau d/\nu$, u_τ is the friction-velocity, d is the channel half-width, and ν is the kinematic viscosity. Hereafter, we normalized the length by d. The flow obeys the incompressible Navier-Stokes equations under periodic boundary conditions with fundamental domain size 2π and π in two wall-parallel directions, the streamwise (x_1) direction and spanwise (x_3) direction respectively. No-slip boundary conditions are imposed on the walls at $x_2 = \pm 1$. The DNS was performed with a spectral method, using Fourier series in the wall-parallel directions and Chebyshev polynomials in the wall-normal direction. In each of the parallel directions, there are 256 equidistant grid points, while in the wall-normal direction, we have 192 Chebyshev grid points. The flow field at one time instant is first interpolated onto 4096 equidistant grid points in the wall-normal direction to ensure that the structures near the walls are sufficiently resolved.

To extract coherent vorticity, an orthogonal anisotropic wavelet decomposition is applied which accounts for the flow anisotropy by using different scales in the wall-normal direction and in the wall-parallel directions. The orthogonal anisotropic wavelets used here combine two-dimensional wavelets $\psi_\alpha(x_1,x_3)$, based on periodized Coiflet 30 wavelets with ten vanishing moments, in the wall-parallel direction and one-dimensional Cohen-Daubechies-Jawerth-Vial (CDJV) interval wavelets $\Psi_\beta(x_2)$, having three vanishing moments (Cohen, Daubechies & Vial, 1993; Cohen, Daubechies, Jawerth & Vial, 1993), in the wall-normal direction. The wavelet transform unfolds any three-dimensional field into scale, positions, and directions. The subscripts (α,β) show the multi-index $(j_h,\mu,j_v,i_1,i_2,i_3)$ denoting the mixed scale $(2^{-j_h},2^{-j_v})$, the position $(2\pi\times 2^{-j_h}i_1, 2\times 2^{-j_v}i_2 - 1, \pi\times 2^{-j_h}i_3)$ and the three directions $\mu = 1,2,3$ of $\psi_\alpha(x_1,x_3)$. Here, $j_h = 0,\cdots,7$, $j_v = j_0,\cdots,11$, $i_n = 0,\cdots,2^{j_h}-1$ $(n = 1,3)$, and $i_2 = 0,\cdots,2^{j_v}-1$. We take j_0 as 3, the minimum number satisfying $2^{j_0-1} \geq M$, where M is the number of the vanishing moments of the CDJV wavelets,

The flow vorticity $\boldsymbol{\omega}$ is then decomposed into orthogonal anisotropic wavelets. The coherent vorticity $\boldsymbol{\omega}_c$ is reconstructed after nonlinearly filtering the wavelet coefficients, namely by retaining only about 0.15% of them that are the most intense. The incoherent vorticity $\boldsymbol{\omega}_i$ is obtained by subtraction, $\boldsymbol{\omega}_i = \boldsymbol{\omega} - \boldsymbol{\omega}_c$. The two fields, $\boldsymbol{\omega}_c$ and $\boldsymbol{\omega}_i$, are orthogonal, which ensures a separation of the total enstrophy into $Z = Z_c + Z_i$. Then we use Biot–Savart's relation $\boldsymbol{U} = -\nabla^{-2}(\nabla\times\boldsymbol{\omega})$ to reconstruct the coherent velocity $\boldsymbol{U}_c$ and the incoherent velocity $\boldsymbol{U}_i$ for the coherent and incoherent vorticity, respectively.

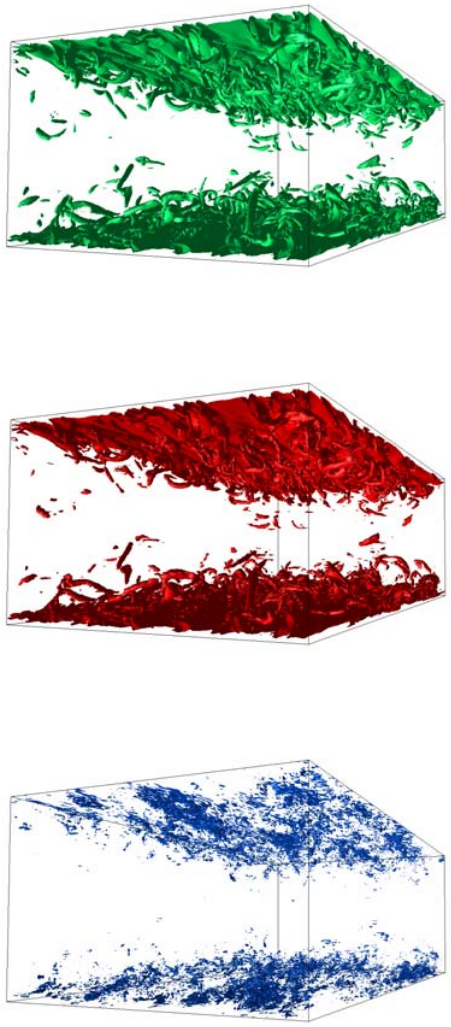

Figure 1. Visualization of total vorticity $\boldsymbol{\omega}^+$ (top), coherent vorticity $\boldsymbol{\omega}_c^+$ (middle) and incoherent vorticity $\boldsymbol{\omega}_i^+$ (bottom). Isosurfaces $|\boldsymbol{\omega}^+| = |\boldsymbol{\omega}_c^+| = 10.0$ and $|\boldsymbol{\omega}_i^+| = 3.5$ are presented, respectively.

NUMERICAL RESULTS

In the numerical results, discussed below, the quantities with the superscript $^+$ are non-dimensionalized by the wall unit u_τ and ν. Figure 1 (top) shows the modulus of vorticity of the total flow. The flow exhibits intense vortex tubes near the walls, as observed in previous numerical experiments (e.g, Blackburn et al., 1996). Isosurfaces of the

Figure 2. Visualization of total vorticity $\boldsymbol{\omega}$ (top), coherent vorticity $\boldsymbol{\omega}_c$ (middle) and incoherent vorticity $\boldsymbol{\omega}_i$ (bottom). Isosurfaces $|\boldsymbol{\omega}^+| = |\boldsymbol{\omega}_c^+| = \langle|\boldsymbol{\omega}^+|\rangle + 3\langle(|\boldsymbol{\omega}^+| - \langle|\boldsymbol{\omega}^+|\rangle)^2\rangle^{1/2}$ and $|\boldsymbol{\omega}_i^+| = \langle|\boldsymbol{\omega}_i^+|\rangle + 3\langle(|\boldsymbol{\omega}_i^+| - \langle|\boldsymbol{\omega}_i^+|\rangle)^2\rangle^{1/2}$ are presented, respectively, where $\langle\cdot\rangle$ shows x_2-dependent spatial average of $\cdot$ over the $x_1 - x_3$ plane.

modulus of the coherent and incoherent vorticity are shown in Figs. 1 (middle) and (bottom), respectively. The value of the isosurface chosen is the same for the total and coherent vorticity, while it has been reduced by about a factor 3 for the incoherent vorticity whose fluctuations are much smaller.

We find that the coherent vorticity represented by 0.15% of the wavelet coefficients $256^2 \times 4096$, i.e., 3.3% of the original grid points $256^2 \times 192$, retains the vortex tubes of the turbulent flow. The coherent flow preserves 99.9% of the total energy and 99.5% of the total enstrophy. In contrast, the incoherent vorticity, which consists of the remaining majority of the coefficients, is structureless. It corresponds to a noise-like incoherent background flow, which has little energy and enstrophy. Figure 2 shows a different

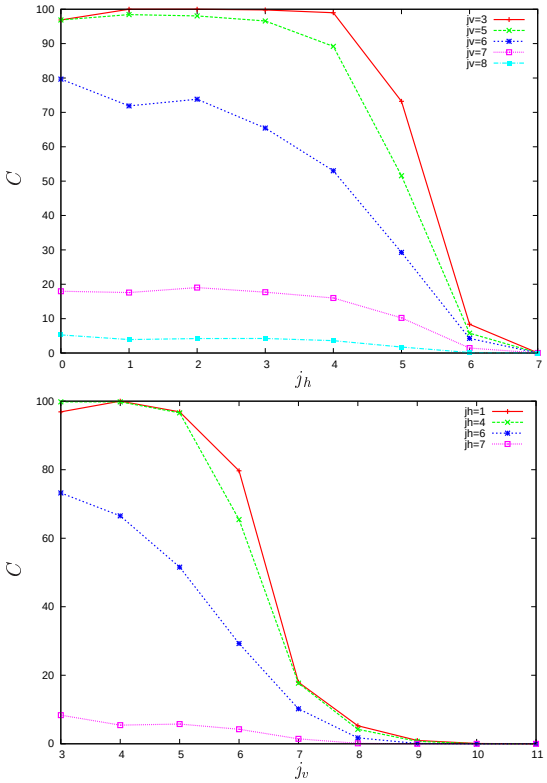

Figure 3. Scale-by-scale compression rates $C(j_h, j_v)$ at the mixed scales (j_h, j_v). (top) $C(j_h, j_v)$ vs. j_h for representative scales j_v, and (bottom) $C(j_h, j_v)$ vs. j_v for representative ones j_h.

type of visualization of vorticity. The vorticity structure in the core region is visualized, using x_2-dependent isosurface values of the modulus of the total, coherent and incoherent vorticity. It is also found that tube-like vortices are well preserved by the coherent vorticity and the incoherent vorticity is almost structureless.

The scale-by-scale compression rate $C(j_h, j_v)$ can be defined by the percentage of coefficients corresponding to the retained coherent part at the mixed scale $(2^{-j_h}, 2^{-j_v})$. In Fig. 3, we find that almost all coefficients are retained at large scales, i.e., for small j_h and small j_v. It is seen that $C(j_h, j_v)$ decays with decreasing scales, i.e., increasing j_h or j_v. The extraction method thus becomes more efficients as the scales become smaller.

Let us decompose the flow velocity $U_j(x_1, x_2, x_3, t)$ as $U_j = \bar{U}_j(x_2, t) + u_j(x_1, x_2, x_3, t)$, where $\bar{U}_j$ is the mean velocity defined by $\bar{U}_j = \langle U_j \rangle$, and u_j is the velocity fluctuation. Here, $\langle\cdot\rangle$ stands for averaging over the $x_1 - x_3$ plane at each x_2. The coherent flow (figure omitted) excellently preserves the mean flow in the streamwise direction, $\bar{U}_1$, while the incoherent mean flow is very weak and thus negligible. In Fig. 4, we show the x_2^+-dependence of the root-mean-square (rms) of u_j^+ $(j = 1, 2, 3)$ for the total, coherent and incoherent flows. The coherent flow well retains the rms values of the total flow. The rms values of the incoherent flow are found to be small enough compared to those of the total one.

Figure 5 shows the energy spectra of total, coherent, and incoherent streamwise-velocity fluctuations, u_1, in its longitudinal direction at a representative location x_2^+ in the

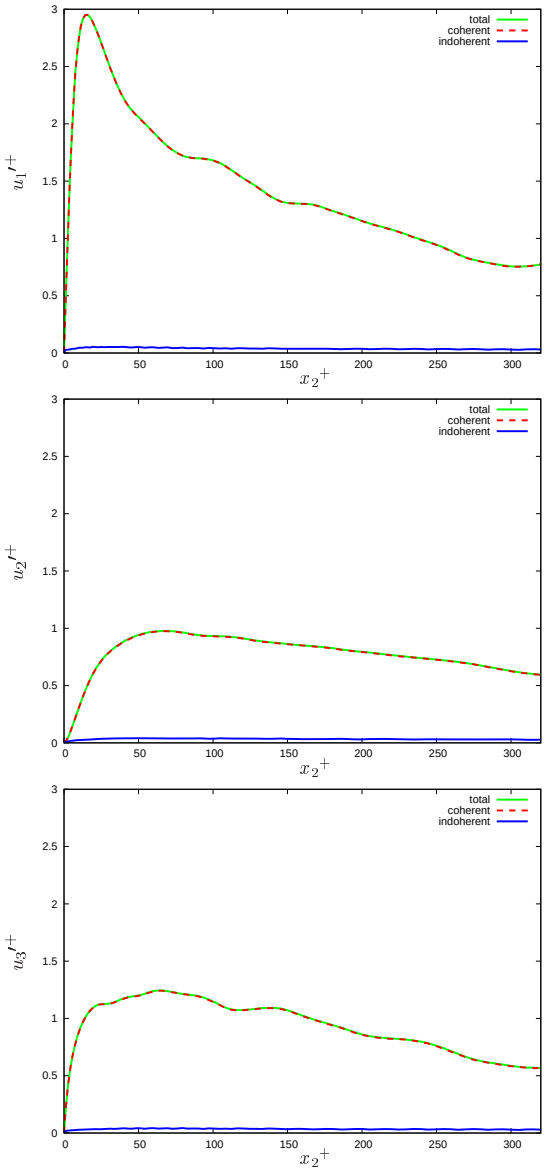

Figure 4. x_2^+-dependence of the root-mean-square of velocity components (u_1^+, u_2^+, u_3^+) for total, coherent and incoherent flows.

core region. The one-dimensional spectrum is denoted by $E(k_1, x_2)$, where k_1 is the wavenumber in the streamwise direction. The coherent energy spectrum is in good agreement with the total one, while the incoherent kinetic energy spectrum is almost flat, that is, close to k^0. This flat spectrum may be attributed to equipartition of incoherent energy that gives rise to spatially decorrelation of the incoherent flow.

Finally, we examine contributions of the coherent flow on the nonlinear dynamics. Figure 6 shows production P, turbulent diffusion T and pressure diffusion Π^d vs. x_2^+ for the total and coherent flows. These quantities are defined in the budget equation for $\langle u_j^+ u_j^+ \rangle / 2$ per unit mass (Mansour et al., 1988):

$$P = -\langle u_j^+ u_l^+ \rangle \partial_l \bar{U}_j^+, \tag{1}$$

$$T = -\frac{1}{2} \partial_l \langle u_j^+ u_j^+ u_l^+ \rangle, \tag{2}$$

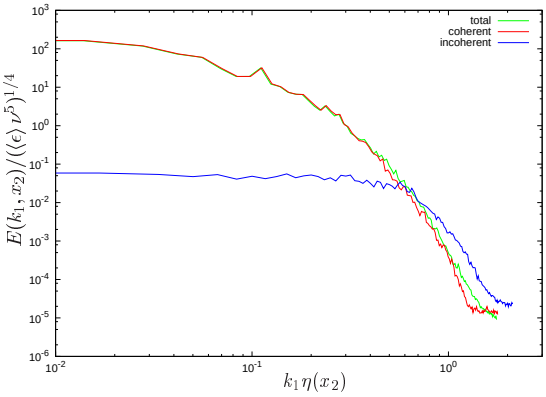

Figure 5. Energy spectra of the streamwise velocity fluctuations in the streamwise direction; $E(k_1, x_2)/\{\langle \varepsilon \rangle \nu^5\}^{1/4}$ vs. $k_1 \eta(x_2)$ at $x_2^+ = 310.6$ in the core region. Here, $\langle \varepsilon \rangle$ is the mean energy dissipation rate per unit mass at x_2 and $\eta(x_2) = \{\nu^3/\langle \varepsilon \rangle\}^{1/4}$. The total, coherent and incoherent spectra are plotted in green, red and blue, respectively.

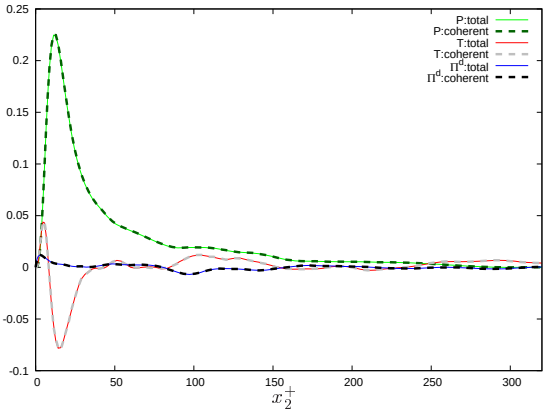

Figure 6. x_2^+-dependence of production P, turbulent diffusion T, and pressure diffusion Π^d for the total and coherent flows.

$$\Pi^d = -\partial_l \langle p^+ u_l^+ \rangle, \tag{3}$$

where $\partial_l = \partial / \partial x_l$, and the repeated subscripts imply summation over $1, 2, 3$. The results show that the nonlinear dynamics measured by these quantities are fully captured by the coherent flow.

CONCLUSION

Coherent vorticity has been extracted out of turbulent channel flow computed at a given time instant, using three-dimensional anisotropic orthogonal wavelets. The coherent vorticity is found to retain the vortex tubes of the turbulent flow while requiring only 3% percent of the degrees of freedom. The remaining majority of the coefficients corresponds to a structureless, i.e., noise-like incoherent background flow. We find that the coherent contributions well preserve not only the turbulent statistics, e.g., energy, enstrophy and energy spectra, but also the nonlinear dynamics

of the flow. This work would be encouraging for developing coherent vorticity simulation (CVS) of turbulence in the presence of walls. CVS is a deterministic computation of the coherent flow evolution using an adaptive orthogonal wavelet basis (Farge and Schneider, 2001). The influence of the incoherent background flow is neglected to model turbulent dissipation. Applications of CVS to turbulent mixing layers and isotropic turbulence can be found in Schneider et al., 2005 and Okamoto et al., 2011, respectively.

ACKNOWLEDGMENT

The computations were carried out on the FX10 systems at the Information Technology Center of Nagoya University. This work was partly supported by JSPS KAKENHI Grant Numbers, (S) 24224003 and (C) 25390149. K.S. thankfully acknowledges financial support from the ANR project SiCoMHD (ANR-Blanc 2011-045).

REFERENCES

Brown, G., and Roshko, A., 1974, "On density effects and large structure in turbulent mixing layers", J. Fluid Mech., Vol. 64, pp. 775−816.

She, Z-S, Jackson, E., and Orszag, S. A., 1991, "Structure and dynamics of homogeneous turbulence: models and simulations", Proc. Math. Phys. Sci., Vol. 434, No. 1890, pp. 101-124.

Farge, M., Pellegrino, G., and Schneider, K., 2001, "Coherent vortex extraction in 3d turbulent flows using orthogonal wavelets", Phys. Rev. Lett., Vol. 87, 45011.

K. Schneider, M. Farge, G. Pellegrino, and M. Rogers, 2005, "Coherent vortex simulation of 3D turbulent mixing layers using orthogonal wavelets", J. Fluid Mech., Vol. 534, pp. 39−66.

Khujadze, G., Nguyen van yen, R., Schneider, K., Oberlack, M., and Farge, M., 2011, "Coherent vorticity extraction in turbulent boundary layers using orthogonal wavelets," Turbulent Boundary Layers, Center for Turbulence Research, Summer Program 2010, Stanford University and NASA-Ames, 87−96.

Jeong, J., Hussain, F., Schoppa, W., Kim J., 1997, "Coherent structures near the wall in a turbulent channel flow," J. Fluid Mech., Vol. 332, pp. 185−214.

Cohen, A., Daubechies, I., and Vial, P., 1993, "Wavelets on the interval and fast wavelet transforms", Appl. Comput. Harmon., Anal., Vol. 1, pp. 54−81.

Cohen, A., Daubechies, I., Jawerth, B., and Vial, P., 1993, "Multiresolution analysis, wavelets and fast algorithms on an interval", C. R. Acad. Sci. Paris Ser. I Math., Vol. 316, pp. 417−421.

Morishita, K., Ishihara, T., and Kaneda, Y., 2011, "Small-scale statistics in direct numerical simulation of turbulent channel flow at high-Reynolds number", J. Phys.: Conference Series, Vol. 318, 022016.

Blackburn, H. M., Mansour, N. N., and Cantwell, B. J., 1996, "Topology of fine-scale motions in turbulent channel flow," J. Fluid Mech., Vol. 310, pp. 269−292.

Mansour, N. N., Kim, J., and Moin, P., 1988, "Reynolds-stress and dissipation-rate budgets in a turbulent channel flow", J. Fluid Mech., Vol. 194, pp. 15−44.

Farge, M., and Schneider, K., 2001, "Coherent Vortex Simulation (CVS), a semi-deterministic turbulence model using wavelets", Flow. Turbul. Combust., Vol. 6, 393−426.

Okamoto, N., Yoshimatsu, K., Schneider, K., Farge M., and Kaneda, Y., 2011, "Coherent vorticity simulation of three-dimensional forced homogeneous isotropic turbulence", SIAM Multiscale Model. Simul., Vol. 9, pp. 1144−1161.